Science of the Total Environment 644 (2018) 862–872

Contents lists available at ScienceDirect

Science of the Total Environment

journal homepage: www.elsevier.com/locate/scitotenv

Boreal forest soil CO_2 and CH_4 fluxes following fire and their responses to experimental warming and drying

Xiaoyan Song [a,b], Genxu Wang [a,*], Zhaoyong Hu [a], Fei Ran [a], Xiaopeng Chen [a,b]

[a] Institute of Mountain Hazards and Environment, Chinese Academy of Sciences, Chengdu 610041, People's Republic of China
[b] University of Chinese Academy of Sciences, Beijing 100049, People's Republic of China

HIGHLIGHTS

- Post-fire boreal forest had higher soil CO_2 flux than the mature forest.
- Fire changed the boreal forest soil from a weak source of CH_4 to a weak sink.
- Warming, drying and their combination made the post-fire soil a stronger C flux.

GRAPHICAL ABSTRACT

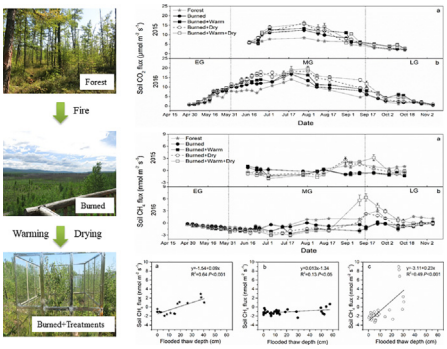

ARTICLE INFO

Article history:
Received 21 April 2018
Received in revised form 1 July 2018
Accepted 1 July 2018
Available online 11 July 2018

Editor: Jay Gan

Keywords:
Soil carbon emissions
Simulated warming
Drying
Permafrost
Post-fire ecosystem

ABSTRACT

Boreal forests store large amounts of organic carbon and are susceptible to climate changes, particularly rising temperature, changed soil water and increased fire frequency. The young post-fire ecosystems might occupy larger proportions of the boreal forests region with the expected increases in fire frequency in the future and change the carbon (C) balance of this region. However, it is unclear how soil C fluxes in the post-fire boreal forest response to the climate changes. Therefore, a two-year field experiment was conducted in a boreal forest to investigate the effects of fire on the soil C (CO_2 and CH_4) fluxes and the responses of these fluxes to simulated warmer and drier climate conditions. The results showed that the boreal forest recovered form wildfire 7–8 years had higher soil CO_2 flux than the mature forest. Furthermore, the treatments of warming, drying and the combination of warming and drying increased growing season cumulative soil CO_2 flux in the post-fire forest by 15.8%, 20.4% and 34.2%, respectively. However, the boreal forest soil changed from a weak CH_4 source to a weak CH_4 sink after fire disturbance. Although CH_4 absorption increased by warming and drying treatments, the interaction of warming and drying led to a decrease in soil CH_4 uptake. The results indicated that the post-fire soil showed CO_2 and CH_4 fluxes with a greater global warming potential than before burning and that the global warming potential of the soil gas fluxes further increased by warming and drying. The predictive power of models of C cycle-climate feedbacks could be increased by incorporating the distinct ecosystem following fire with permafrost degradation and climate change across the boreal zone.

* Corresponding author.
E-mail address: wanggx@imde.ac.cn (G. Wang).

https://doi.org/10.1016/j.scitotenv.2018.07.014
0048-9697/

1. Introduction

In the high-latitude regions of the earth, temperatures have risen 0.6 °C per decade over the last 30 years, which is twice as fast as the global average (IPCC, 2013), and this trend will likely continue in the future (Overland, 2014). Climate warming in these regions may have biogeochemical consequences because these regions contain large stocks of soil organic matter (Hugelius et al., 2014; Tarnocai et al., 2009), especially the boreal forests, which store 1095 Pg of C, representing more than one-third of global terrestrial C stocks (Bradshaw and Warkentin, 2015).

In boreal forest under a warmer climate, soil C releases are likely to increase due to stimulated soil microbial activities, particularly in association with soil warming and permafrost thawing (Jorgenson et al., 2001; O'Donnell et al., 2012; Kim, 2015; Schädel et al., 2016). The extent of permafrost is expected to continue to decline with future warming (Lawrence et al., 2012; Slater and Lawrence, 2013), which can release a large amount of thermally protected C (permafrost C) to the atmosphere (Lawrence et al., 2012; Schuur et al., 2008; Schuur et al., 2013; Slater and Lawrence, 2013), further amplifying climate change (Macdougall et al., 2012). Moreover, the potential loss of soil C to the atmosphere is also driven by the soil hydrological processes which associated with the local hydrological and topographical conditions (Morgenstern et al., 2013) and the changes in the precipitation patterns (Bintanja and Selten, 2014; Held and Soden, 2006). Although the increase in the soil CO_2 flux in response to a warmer climate may be limited by saturated soil conditions (Lawrence et al., 2015), such conditions are expected to decrease in some areas in the future because of permafrost degradation (Avis et al., 2011; Lawrence et al., 2015), forming stronger positive feedbacks on climate (Lawrence et al., 2015; Schädel et al., 2016). On the other hand, the production of CH_4, a powerful greenhouse gas (IPCC, 2013), might be limited by the drainage of water following permafrost thaw, leading to negative feedbacks. Therefore, how the soil C flux responds to combined warming and drying is closely related to the form of C (CO_2 or CH_4) released to the atmosphere, but few studies have focused on both CO_2 and CH_4 fluxes (Natali et al., 2015; Updegraff et al., 2001). Artificially drained or lowered water tables have been shown to result in a consistent increase in soil CO_2 release (Merbold et al., 2009) or a reduction in CH_4 fluxes during the growing season (Merbold et al., 2009; Kim, 2015; Kwon et al., 2017; Sturtevant et al., 2012) due to more oxic conditions and shifts in microbial activity and community structure. These results are the same for the predicted results of soil C fluxes with decreased soil water when permafrost thaws (Lawrence et al., 2015). However, how soil drying combined with warming affects soil CO_2 and CH_4 fluxes is still unclear due to the limited number of *in situ* experiments manipulated both moisture and temperature (Chivers et al., 2009; Natali et al., 2015; Turetsky et al., 2008; Updegraff et al., 2001).

Boreal forests are also strongly affected by wildfires, which instantaneously release large amounts of C to the atmosphere from combustion (Mack et al., 2011). Following fire, the ecosystem C balance was presumably altered due to the changes of surface reflectance, energy partitioning, and because the reducing of soil organic layer insulating permafrost led to thaw and destabilization of the ground surface (Mack et al., 2011). The boreal forests would act as C sources about 10 years following fire disturbance until a C compensation point where net ecosystem production (NEP) becomes positive is reached (Amiro et al., 2015; Kurz et al., 2013). Meanwhile, these young post-fire forests will occupy a larger fraction of the boreal regions due to the increased effects of fire under climate change (Abbott et al., 2016). Furthermore, the long-term recovery of C balance and organic carbon stocks in the burned forest are likely to be primarily driven by the warming climate (Jiang et al., 2016). Therefore, it is important to understand the post-fire soil C fluxes and their responses to climate changes (such as climate warming and dryer soil conditions) when predicting the C balance of boreal regions in the future. Although the young post-fire boreal forest with changed vegetation and soil microbial communities, modified soil nutrient availability and induced permafrost degradation might be more sensitive to perturbations than mature systems based on the feature of ecosystem (Kröel-Dulay et al., 2015) and interact with climate changes (Allison et al., 2010; Brown et al., 2015; Jiang et al., 2016; Kim and Tanaka, 2003), the knowledge of how post-fire boreal forest soil CO_2 and CH_4 fluxes response to warming and drying is still limited.

Therefore, we examined the soil C fluxes of a young post-fire boreal forest and their responses to combined warming and drying, which are the key climate change processes in the boreal permafrost region. This work was conducted in a continuous permafrost region of the DaXing'anling Mountains, which plays an important role in the C budget of China (Fang et al., 2001). Because this region is at the southern boundary of the boreal forests, the study area is extremely sensitive to climate change (Peng et al., 2009). We hypothesized that 1) soil CO_2 flux in the post-fire boreal forest would be higher than that in the mature forest and further increased by warming and drying, but 2) soil CH_4 flux in the post-fire forest would be lower than that in the mature forest and further decreased by warming and drying.

2. Materials and methods

2.1. Study site

The experiment was located in the northern DaXing'anling Mountains (51.892° N, 121.912° E, 654 m a.s.l.), Northeast China. The study site is situated in the continuous permafrost zone. The annual average precipitation of the study area is approximately 500 mm, >60% of which occurs between June and August. The annual average temperature is −3.6 °C, with an average of −29.8 °C in the coldest month, January, and an average of 18.1 °C in the hottest month, August. Therefore, it has a terrestrial monsoon climate. The soil type is classified as Gelisols according to the USDA or as Crysols in the WRB scheme (Bockheim, 2015), and the details of the soil properties are shown in Supplementary Table A. The soil has an organic horizon that is 35 ± 2 cm thick above the mineral soil. The active layer, which thaws annually during the growing season, reaches a maximum depth of 44 ± 3 cm, below which is the perennially frozen permafrost layer. The vegetation of this area is classified as cool temperate coniferous forest in the southern extent of the eastern Siberian boreal forests (Wang et al., 2001).

In 2008, an extremely intense fire caused by lightning strikes burned approximately 478 ha of mature *Larix gmelinii* forest (117 ± 5 years) and resulted in most mortality of the overstory and ground cover and combustion of approximately 5 cm of the forest floor. Six years after the wildfire, many of the dead trees were still standing, and many shrubs <2 m (such as *Alnus hirsuta*, *Betula fruticosa*, *Ledum palustre* and *Vaccinium uliginosum*), grasses (such as *Calamagrostis* and *Carex*) and mosses (such as *Sphagnum* and *Polytrichum*) had recovered. The warming and drying experiment is situated in this fire scar (Supplementary Fig. A) in a relatively well-drained depression. To investigate the fire effects, we chose a comparable un-burned forest site (Supplementary Fig. B) that was adjacent to the burned site (<1 km) and that had a similar environmental conditions and similar vegetation composition to the burned site before the fire. The mature forest was located in a depression. The tree layer was dominated by *Larix gmelinii* with a canopy density of 0.6, density of 625 trees ha^{-1}, mean height of 16.4 m and mean diameter at breast height of 17.1 cm. The shrub layer was dominated by *Ledum palustre*; and the ground cover was dominated by *Sphagnum*, *Calamagrostis* and *Carex*.

2.2. Experimental design

We had a total of five treatments (forest, burned, burned + warm, burned + dry and burned+warm+dry) with six replicates of each

treatment in this experiment (30 plots in total). In the forest site, six replicates were randomly distributed with distances of at least 6–8 m. A factorial design of warming and drying treatments was established in the burned site in June 2014. The drying treatment was established using drainage channels, which were 30 cm wide, 40 cm deep and approximately 80 m long. The drying treatment changed the soil surface temperature, moisture and the water table dynamics during the growing season (Table 1; Supplementary Fig. C, D). The blocks with the drying treatment were approximately 20 m away from the no-drying blocks. Twelve artificial warming treatment plots with open-top chambers (OTCs) were installed, 6 of which were established in the drying treatment block, and the other 6 were established in the no-drying blocks with a distance of at least 6–8 m. The warming treatment was achieved by using 2 m × 2 m × 2 m OTCs as passive warming devices to generate an artificially warmed environment (Marion et al., 1997). The cubic OTCs were made of 5-mm-thick translucent synthetic glass with high solar transmittance in the visible wavelengths (approximately 90%) and low transmittance in the infrared (heat) range (<5%). The OTCs increased air temperatures by approximately 1 °C in the growing season (Table 1; Supplementary Fig. C). Plots (2 m × 2 m) that were not warmed were established near each OTC at a distance of approximately 3 m.

2.3. Soil CO_2 and CH_4 measurements

We randomly selected 5 locations within each plot for soil CO_2 and CH_4 flux measurement. Soil CO_2 and CH_4 fluxes were measured using an Ultra-portable Greenhouse Gas Analyzer (UGGA) that consisted of a laser off-axis integrated cavity output spectroscopy analyzer (Los Gatos Research, CA, USA). Before the measurements, polyvinyl chloride collars (21.4 cm in diameter and 15 cm in height) were inserted into the soil to a depth of approximately 10 cm in each plot. Small grasses and seedlings that grew within the collars were clipped to remove the effect of aboveground plant respiration (Webster et al., 2008). The concentrations of CH_4, H_2O, and CO_2 and the air temperature and pressure inside the chambers were recorded at a 5-s rate, and data acquisition continued for 300 s for each chamber. When calculating the soil CH_4 and CO_2 fluxes, the first 50 s and the last 30 s of gas concentration data were excluded. More details on the measurements were previously described in Song et al. (2017).

Based on the diurnal patterns of soil CO_2 and CH_4 fluxes at this site (Song et al., 2017), the measurements of soil CO_2 and CH_4 fluxes were taken between 08:00 and 11:00 local time, which represented the daily mean flux. The measurements were taken from June to October in 2015 and from May to November in 2016. We divided the entire growing season into three periods according to the soil temperature of the mature forest at a depth of 5 cm: early growing season (EG: from May 1 to June 1; the thaw process, the soil temperature increased from 0 to 5 °C); middle growing season (MG: from June 1 to October 1; the soil temperature was >5 °C); and late growing season (LG: from October 1 to November 10; the freeze process, the soil temperature decreased from 5 to 0 °C) (Chen et al., 2017). Soil CO_2 and CH_4 fluxes were measured twice per week in the EG, and once per week in the MG and LG, for a total of 45 measurements at each plot.

2.4. Auxiliary measurements

Air temperature, relative humidity, photosynthetically active radiation (PAR) (1 m above ground), soil temperature and soil moisture at 5 cm soil depth were recorded by data loggers (CR1000; Campbell, USA) that were installed in the plots of each treatment without flux measurement collars. Meanwhile, the soil temperature at a depth of 5 cm and the soil volumetric water content at 0–10 cm were measured near the collar simultaneously with the soil C flux measurements to obtain more accurate soil environment factors of each plots. The soil temperature was measured with a thermocouple probe connected to the UGGA. The soil volumetric water content was measured using a portable MST3000+ (STEP Systems GmbH, Essen, Germany) when the soils were thawed down to 15 cm. Water tables were measured in parallel with flux measurements within permanently installed perforated polyvinyl chloride pipes (ø 40 mm) in the burned + dry plots and burned plots. Water table depth was the distance from the ground to the water table surface, with values <0 cm denoting water standing below the soil surface. The thaw depth was measured at the same time as the flux measurements by pushing a measuring pole (ø 5 mm) into the ground in each plot away from collars.

Soil organic carbon (SOC) and total nitrogen (TN) content were measured by a Vario Macro cube (Elementar, Langenselbold, Germany) analyzer. The organic carbon content was assumed to be equal to the total carbon content because of the absence of carbonates in the acidic (pH < 6.8) soils. Soil samples collected from the 0–15 cm horizon in August 2016 were analyzed soil microbial biomass carbon (MBC), microbial biomass nitrogen (MBN), dissolved organic carbon (DOC), dissolved total nitrogen (DTN) and four soil enzymatic activities related to the soil C cycle. The soil MBC and MBN were analyzed by the chloroform fumigation extraction method (Wu et al., 1990), and the organic C and N contents in the samples without fumigation were used as the soil DOC and DTN. Soil β-glucosidase activity was assayed by hydrolyzing para-nitrophenyl-β-D-glucopyr-anoside (Eivazi and Tabatabai, 1988). Soil invertase and amylase activities were determined using sucrose and amylum as substrate, respectively (Guan et al., 1986). The analysis of acid phosphatase activity involved *p*-nitrophenyl phosphate and essentially followed the method of Guan et al. (1986). Fine roots (<2 mm in diameter) (Lee and Jose, 2003) at 0–10 and 10–20 cm depths were sampled once in August 2016. We washed the samples and collected as many of the fine roots as possible (90%) using tweezers, and then, we weighed them after drying them for 48 h at 65 °C.

Table 1
Experimental treatment effects on environment conditions[§].

	Forest	Burned	Burned + warm	Burned + dry	Burned + warm + dry
Air temperature (°C)[€]	ND[◎]	7.62	8.36	7.69	8.68
Soil temperature (°C)[※]	5.23 ± 0.16[€]	5.37 ± 0.14[€]	5.38 ± 0.14[€]	5.97 ± 0.04[§]	5.91 ± 0.13[§]
Soil moisture (%)[¤]	25.54 ± 1.71[€]	45.52 ± 2.31[§]	38.16 ± 6.82[§]	25.36 ± 2.47[€]	19.52 ± 1.05[€]
Average thaw depth (cm)[#]	26.0 ± 0.8[€]	29.7 ± 1.2[§]	29.9 ± 0.8[§]	29.7 ± 0.6[§]	27.4 ± 0.4[€]
Maximum thaw depth (cm)[&]	46.0 ± 1.0[¤]	62.4 ± 1.2[§€]	65.1 ± 1.2[§]	57.5 ± 1.8[€※]	55.2 ± 1.6[※]
Average water table (cm)[@]	−17.5	−20.0	ND	−26.3	ND

[§] Same letter in a row denotes non-significant differences among treatments from *post hoc* comparison of mean tests at $P \geq 0.05$.
[€] 1 m height from ground, measured from 1 May to 1 November in 2015 and 2016 (Mean, n = 1).
[※] Soil temperature from a 5 cm depth, measured from 1 May to 17 October in 2015 and 2016 (Mean ± Se, n = 5).
[¤] Volumetric water content from a 0–15 cm depth; measured from 19 May to 1 October 2015 and 2016 (Mean ± Se, n = 5).
[#] Measured from 1 May to 1 October in 2016 (Mean ± Se, n = 5).
[&] Measured from 1 October in 2016 (Mean ± Se, n = 5).
[@] Distance from the ground to water table surface, with values <0 cm denoting water standing under the soil surface, 1 June to 1 October in 2016 (Mean, n = 1).
[◎] Not detected.

2.5. Statistical analysis

The temperature sensitivity of the soil CO_2 flux ($Q_{10} = e^{10b}$) was calculated for each chamber using the van't Hoff equation ($y = \alpha e^{bt}$) (Lloyd and Taylor, 1994). Cumulative soil CO_2 and CH_4 fluxes for each plot were obtained by interpolating the soil CO_2 and CH_4 fluxes between sampling dates and then computing the sum of the average fluxes as follows (Zhang et al., 2015):

$$F_C = \sum F_{m,k}\Delta t_k$$

where F_C is the cumulative soil CO_2 or CH_4 flux in the sampling period; $\Delta t_k = (t_k - t_{k-1})$ is the time sequence of the field measurements across the study period; and $F_{m,k}$ is the average soil CO_2 or CH_4 flux over the interval (t_{k-1}, t_k). The boreal forests following fire can uptake carbon and emit methane (Song et al., 2017), and thus have both cooling and warming impacts on the climate system through their influence on atmospheric burdens of CO_2 and CH_4. These competing impacts are usually compared by the global warming potential (GWP), which determines the equivalent annual CO_2 emission that would have the same integrated radiative forcing impact over a chosen time horizon as the annual CH_4 emission. We converted CH_4-C into CO_2-C equivalent by multiplying CH_4-C by its latest consensus GWP of 34 on a 100-year timescale (IPCC, 2013). Therefore, GWP of the total C flux in each treatment was calculated by summing up the cumulative soil CO_2 flux and 34 times of the cumulative CH_4 flux (IPCC, 2013).

Soil CO_2 and CH_4 fluxes were analyzed with repeated-measures ANOVA with the date of measurement as within-subject comparisons and fire and topography as fixed effects. One-way ANOVA was used to test the differences of the cumulative soil C flux, Q_{10}, soil environment factors, soil properties, soil enzymatic activities and fine root biomass among all treatments. The relationships between the soil C fluxes and soil environment factors were assessed by regression analysis. The correlations between soil C fluxes and soil properties, enzymatic activities and fine root biomass were analyzed by Pearson correlation with two tails. SPSS 19.0 (SPSS Inc., Chicago, IL, USA) was used for statistical analyses with a significance level of 0.05.

3. Results

3.1. Environmental variables

After the recovery of fire 7–8 years, the burned site had significant higher soil moisture values and a deeper thaw depth and water table than the mature forest (Table 1; Supplementary Fig. C, D). After simulated warming treatment, the mean air temperature in the burned + warm plot was 0.74 °C higher than that of the burned plots. Similarly, the burned + warm + dry plots had a higher mean air temperature of 0.99 °C than the burned + dry plots (Table 1; Supplementary Fig. C). However, the mean soil temperature at a depth of 5 cm was not significantly changed by warming treatment but significantly increased by drying treatment (Table 1; Supplementary Fig. C). At the same time, the soil volumetric water content at a 0–15 cm depth significantly decreased under the warming and drying treatments, with a 16.2% lower volumetric water content in the burned + warm plots, a 44.3% lower content in the burned + dry plots and a 57.1% lower content in the burned + warm + dry plots than the burned plots (Table 1; Supplementary Fig. C). While simulated drying treatments increased soil temperatures and decreased soil moistures, there were shallower maximum thaw depths (active layer depth) under drying condition (Table 1); specifically, the active layer depth was 7.9% shallower in the burned + dry plots than in the burned plots, and that was 11.5% shallower in the burned + warm + dry plots than in the burned + warm plots (Table 1). Moreover, the burned + dry plots had a deeper water table than the burned plots (Table 1; Supplementary Fig. D).

3.2. Soil characteristics and enzymatic activities

Although the soil MBC, MBN and DOC contents were lower following the fire, the burned site had relative higher soil enzymatic activities than the mature forest (Fig. 1). Under the warming and drying treatments, the soil MBC, DOC, DON contents and invertase and amylase activity of this early successional ecosystem did not change, but the soil MBN content, MBC/MBN ratio, β-glucosidase and acid phosphatase activities significantly changed (Fig. 1). The burned + warm + dry plots had significantly lower soil MBN contents and therefore higher MBC/MBN ratios than the burned plots (Fig. 1). There was a decreasing trend for soil β-glucosidase in the burned + dry plots, and for acid phosphatase activities (Fig. 1). Following recovery over 8 years, the burned sites still had lower fine root biomasses at both 0–10 cm and 10–20 cm soil depths than the mature forest, and the fine root biomass at 0–10 cm decreased further in the burned + dry and burned+warm+dry plots (Supplementary Fig. E).

3.3. Soil CO_2 flux

Soil CO_2 flux of the burned plots was significantly higher than that of the mature forest and increased further under simulated warming and drying (Fig. 2; Table 2; Table 4). Throughout the entire growing season, cumulative soil CO_2 flux in the forest was significantly increased by wildfire by 27.0%. Furthermore, warming and drying significantly increased the mean soil CO_2 flux. When combined with the date, only drying treatment condition had a higher soil CO_2 flux (Fig. 2; Table 2). But, there were no interactive effects between warming and drying on the soil CO_2 flux (Table 2). Specifically, the burned + warm, burned + dry and burned + warm + dry plots had a 15.8%, 20.4% and 34.2% higher total cumulative CO_2 fluxes than the burned plots, respectively (Table 4). Moreover, the soil CO_2 flux showed a higher Q_{10} in the burned site (3.83 ± 0.12) than that in the mature forest (2.55 ± 0.07) ($P < 0.05$; Supplementary Fig. F). However, the Q_{10} of soil CO_2 flux was significantly decreased after warming (3.36 ± 0.11), drying (2.85 ± 0.11) and combined warming and drying treatments (2.65 ± 0.12; $P < 0.05$; Supplementary Fig. F).

Soil CO_2 flux significantly varied with date (Table 2) and showed similar seasonal variation at all sites (Fig. 2). Meanwhile, the treatment effects on soil CO_2 flux were different among periods. The significant warming effects were found in the EG and LG, whereas the significant drying effects were found in the MG and LG (Table 2). Although the cumulative soil CO_2 fluxes of the LG period were lower than those of the EG and MG periods, the differences in the cumulative soil CO_2 fluxes between the treatments and burned plots were highest in the LG period (Table 4). Specifically, the cumulative soil CO_2 fluxes of the burned + warm plots were 21.3%, 10.2% and 63.9% higher than those in the burned plots in the EG, MG and LG periods, respectively (Table 4). For the burned + dry plots, the cumulative soil CO_2 fluxes were 11.6%, 21.0% and 27.9% higher than those in the burned plots in the EG, MG and LG periods, respectively (Table 4). For the burned + warm + dry plots, the cumulative soil CO_2 fluxes were 23.8%, 32.3% and 69.2% higher than those in the burned plots in the EG, MG and LG periods, respectively (Table 4).

Cumulative soil CO_2 fluxes of all plots were negatively correlated to soil MBC and MBN but positively correlated to DTN and Amylase and Acid phosphatase activities of August 2016 (Supplementary Table B). Over the entire growing season, soil CO_2 fluxes were mostly associated with the 5 cm soil temperature ($R^2 = 0.64$), ground thaw depth ($R^2 = 0.61$), flooded thaw depth ($R^2 = 0.40$) and water table depth ($R^2 = 0.39$; Table 3). However, there were different correlations between the soil environment factors and the soil CO_2 flux in the EG, MG and LG periods (Table 3) due to the distinct environmental conditions. Soil CO_2 flux was primarily controlled by thaw depth and temperature in the EG and LG period, whereas it was strongly affected by water table and thaw depth in the MG period (Table 3).

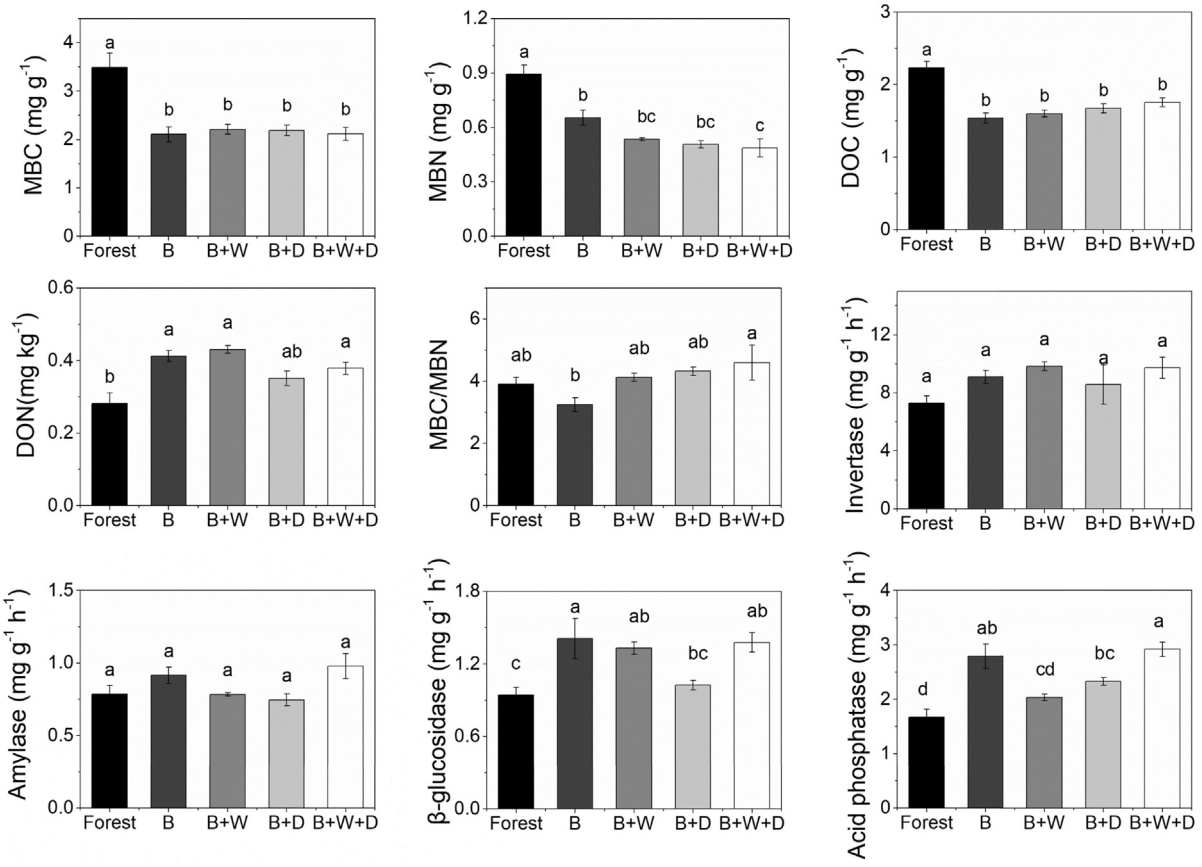

Fig. 1. Soil microbial biomass carbon (MBC), microbial biomass nitrogen (MBN), dissolved organic carbon (DOC), dissolved total nitrogen (DTN), MBC/MBN ratio and soil enzymatic activities at a 0–15 cm soil depth in the forest, burned (B), burned + warm (B + W), burned + dry (B + D) and burned + warm + dry (B + W + D) sties. Error bars represent standard error of the mean (n = 5).

3.4. Soil CH_4 flux

Fire significantly affected the soil CH_4 flux of the forest (Table 2) and changed the mature forest soil from a weak source of CH_4 to the atmosphere to a weak sink (Table 4). For the burned ecosystem, separate warming and drying had no significant effect on soil mean CH_4 flux, but there was a significant interaction of warming and drying on soil mean CH_4 flux. Based on the entire growing season, the effects of warming, drying and their interaction on the soil CH_4 flux were all significant (Table 2). Specifically, the cumulative soil CH_4 uptakes

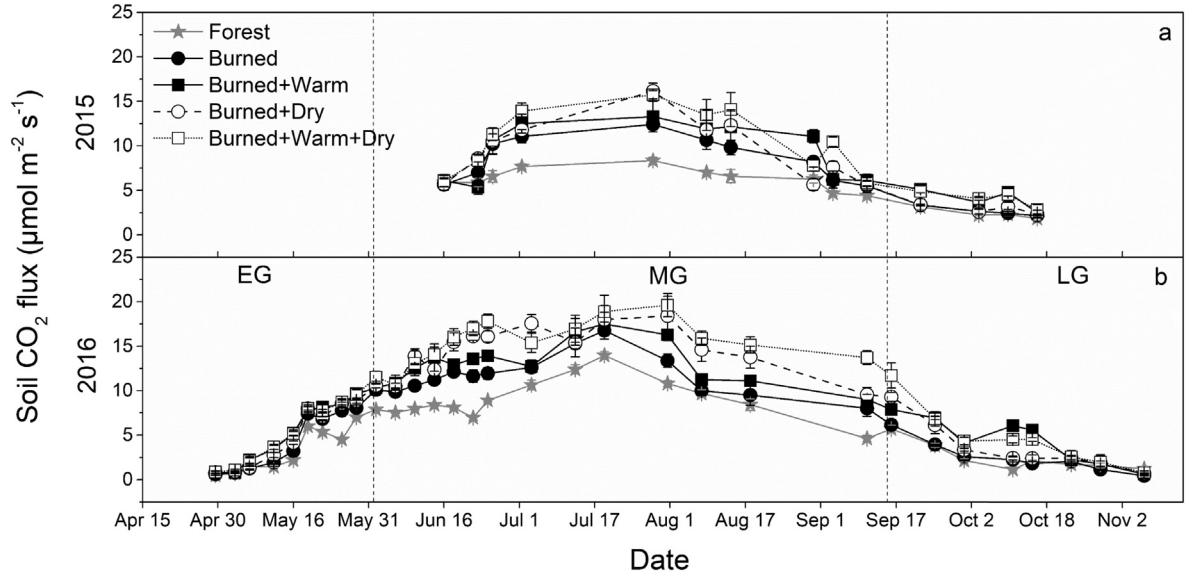

Fig. 2. Seasonal variation of soil CO_2 flux in the forest, burned, burned + warm, burned + dry and burned + warm + dry sites in 2015 (a) and 2016 (b). Error bars represent standard error of the mean (n = 5); EG, MG and LG represent the early, middle and late growing season, respectively.

Table 2
Repeated-measures ANOVA results of soil CO_2 and CH_4 fluxes.

Period[§]		Soil CO_2 flux			Soil CH_4 flux		
		df	F	*P*	df	F	*P*
G	Fire	1	20.684	<**0.01**	1	20.171	<**0.01**
	Date × fire	44	9.833	<**0.01**	44	13.841	<**0.01**
	Warm	1	8.149	<**0.05**	1	0.411	0.530
	Dry	1	9.941	<**0.01**	1	3.926	0.065
	Warm × dry	1	0.167	0.688	1	6.800	<**0.05**
	Date	44	212.826	<**0.01**	44	38.850	<**0.01**
	Date × warm	44	1.885	0.077	44	5.175	<**0.01**
	Date × dry	44	5.933	<**0.01**	44	25.927	<**0.01**
	Date × warm × dry	44	0.880	0.526	44	5.182	<**0.01**
EG	Warm	1	13.188	<**0.01**	1	6.600	<**0.05**
	Dry	1	1.949	0.182	1	2.794	0.114
	Warm × dry	1	1.412	0.252	1	0.721	0.216
	Date	8	865.843	<**0.01**	8	29.449	<**0.01**
	Date × Warm	8	5.239	<**0.01**	8	0.255	0.914
	Date × Dry	8	0.968	0.435	8	0.442	0.788
	Date × Warm × Dry	8	0.620	0.662	8	0.975	0.430
MG	Warm	1	3.730	0.071	1	10.401	<**0.01**
	Dry	1	11.687	<**0.01**	1	1.546	0.232
	Warm × dry	1	0.014	0.907	1	2.729	0.071
	Date	23	65.085	<**0.01**	23	34.121	<**0.01**
	Date × warm	23	1.490	0.183	23	4.229	<**0.01**
	Date × dry	23	5.259	<**0.01**	23	22.898	<**0.01**
	Date × warm × dry	23	0.967	0.456	23	5.325	<**0.01**
LG	Warm	1	26.469	<**0.01**	1	2.906	0.108
	Dry	1	3.040	0.100	1	21.123	<**0.01**
	Warm × dry	1	1.055	0.320	1	8.380	<**0.05**
	Date	8	86.452	<**0.01**	8	34.747	<**0.01**
	Date × warm	8	4.861	<**0.01**	8	5.973	<**0.01**
	Date × dry	8	5.314	<**0.01**	8	32.632	<**0.01**
	Date × warm × dry	8	1.045	0.392	8	4.332	<**0.01**

Significant factors are marked in bold ($P < 0.05$ and $P < 0.01$).
§ G, EG, MG and LG represent the entire and the early, middle and late period of the growing season, respectively.

increased in burned + warm and burned + dry treatments but decreased in burned + warm + dry treatment by 43.6% (Table 4).

Soil CH_4 fluxes significantly varied with date (Fig. 3; Table 2) and showed a peak in September in the forest, burned + dry and burned + warm + dry plots, but there was no obvious seasonal variation in CH_4 fluxes in the burned and burned + warm plots (Fig. 3). So, the treatment effects on soil CH_4 flux were different among periods (Table 2). Soil mean CH_4 fluxes were significantly affected by warming treatment in the EG and MG periods but affected by drying treatment and the interaction of warming and drying in the LG period (Table 3). Specifically, in the EG and MG periods, the burned + warm, burned + dry and burned + warm + dry plots had higher cumulative soil CH_4 uptakes than the burned plots (Table 4). However, in the LG period, cumulative soil CH_4 fluxes in the burned + dry and burned + warm + dry plots were turned into emissions (Table 4).

Cumulative soil CH_4 fluxes of all plots were positively correlated to soil MBC and DOC of August 2016 (Supplementary Table B). Based on all sampling dates, the soil CH_4 flux was highly controlled by flooded thaw depth in the forest ($R^2 = 0.64$; Fig. 4a) and drying treatment (the burned + dry and burned + warm + dry plots; $R^2 = 0.49$; Fig. 4c). Across all sampling dates and plots, soil CH_4 fluxes were associated with the thaw depth ($R^2 = 0.19$), flooded thaw depth ($R^2 = 0.18$) and soil temperature at 5 cm depth ($R^2 = 0.06$; Table 3). For different periods in the growing season, soil CH_4 flux was mostly correlated to ground thaw depth ($R^2 = 0.37$) and soil temperature at 5 cm depth ($R^2 = 0.37$) in the EG period but strongly affected by flooded thaw depth ($R^2 = 0.49$) and water table ($R^2 = 0.38$) in the LG period (Table 3).

3.5. Global warming potentials of soil total C flux

The boreal forest recovered from fire 7–8 years had a global warming potential of soil C flux that was 26.6% higher than that of the

Table 3
Dependence of soil CO_2 and CH_4 fluxes on soil temperature at a 5 cm depth (T), soil moisture at a 0–15 cm depth (M), thaw depth (D), water table (W) and flooded thaw depth (F).

Gas[§]	Period[€]	Factors[※]	Equation	n	R^2	*P*
CO_2	G	T	$Flux = 2.638e^{0.161T}$	1017	0.64	<0.001
		D	$Flux = -3.899 + 0.963D - 0.013D^2$	650	0.61	<0.001
		F	$Flux = 14.058 - 0.184F$	85	0.40	<0.001
		W	$Flux = 5.000 - 0.283W$	85	0.39	<0.001
		M	$Flux = 10.220 - 0.032M$	780	0.01	<0.001
	EG	D	$Flux = -1.947 + 0.585D$	225	0.80	<0.001
		T	$Flux = 1.186e^{0.477T}$	225	0.73	<0.001
	MG	W	Flux =7.589–0.219W	70	0.42	<0.001
		T	$Flux = 4.917e^{0.089T}$	592	0.15	<0.001
		F	$Flux = 13.987 - 0.125F$	70	0.17	<0.001
		D	$Flux = -1.974 + 0.853D - 0.011D^2$	350	0.20	<0.001
		M	$Flux = 13.140 - 0.050\ M$	500	0.04	<0.001
	LG	T	$Flux = 2.964e^{1.870T}$	200	0.53	<0.001
		D	$Flux = -50.558 + 2.084D - 0.019D^2$	75	0.11	<0.05
		M	$Flux = 3.527 + 0.023M$	175	0.03	<0.05
CH_4	G	D	$Flux = 0.241 - 0.095D + 0.002D^2$	650	0.19	<0.001
		F	$Flux = -1.547 + 0.055F$	85	0.18	<0.001
		T	$Flux = -0.091 - 0.091T$	1017	0.06	<0.001
	EG	D	$Flux = -0.221 - 0.061D$	225	0.37	<0.001
		T	$Flux = -0.555 - 0.168T$	225	0.37	<0.001
	MG	F	$Flux = -1.842 + 0.048F$	70	0.19	<0.001
		D	$Flux = -1.704 - 0.017D + 0.001D^2$	350	0.10	<0.001
		T	$Flux = 0.263 - 0.132\ T$	592	0.05	<0.001
	LG	F	$Flux = 8.118 - 0.155F$	15	0.49	<0.01
		W	$Flux = -0.678 - 0.167\ W$	15	0.38	<0.05
		D	$Flux = -12.250 + 0.641D - 0.007D^2$	75	0.18	<0.01
		T	$Flux = 0.235 + 0.247T$	200	0.08	<0.001
		M	$Flux = 1.252–0.020M$	175	0.04	<0.01

§ The units of the soil CO_2 and CH_4 fluxes were μmol m^{-2} s^{-1} and ηmol m^{-2} s^{-1}, respectively.
€ G, EG, MG and LG represent the entire and the early, middle and late period of the growing season, respectively.
※ The dependence of soil CO_2 and CH_4 fluxes on the water table and flooded thaw depth were calculated with the mean of each treatment for all sampling date.

Table 4
Cumulative soil CO_2, CH_4 flux and global warming potential (GWP) of the total C flux for growing season (G), early growing season (EG), middle growing season (MG) and late growing season (LG) in each site (n = 5)[§].

Sites[€]	Cumulative soil CO_2 flux (g C m^{-2})				Cumulative soil CH_4 flux (g C m^{-2})				GWP (g C m^{-2})
	G	EG	MG	LG	G	EG	MG	LG	G
Forest	**1024.5 ± 29.8**[※]	120.9 ± 3.3[※]	807.29 ± 25.3[※]	95.8 ± 4.5[€]	**0.015 ± 0.013**[§]	−0.026 ± 0.001[§€]	−0.011 ± 0.008[§]	0.053 ± 0.005[§]	**1025.1 ± 29.6**[※]
B	**1301.1 ± 59.0**[€]	156.4 ± 6.8[€]	1040.9 ± 45.1[€]	103.6 ± 7.7[€]	**−0.094 ± 0.022**[€※]	−0.025 ± 0.006[§]	−0.054 ± 0.012[§€]	−0.015 ± 0.008[€]	**1297.8 ± 59.0**[€※]
B + W	**1506.8 ± 58.5**[§€]	189.8 ± 9.8[§]	1147.2 ± 47.1[€]	169.8 ± 8.4[§]	**−0.195 ± 0.021**[※]	−0.038 ± 0.002[§€]	−0.127 ± 0.012[※]	−0.029 ± 0.011[€]	**1500.2 ± 58.4**[§€]
B + D	**1566.8 ± 96.9**[§€]	174.5 ± 8.3[§€]	1259.8 ± 84.4[§€]	132.5 ± 9.4[§€]	**−0.111 ± 0.014**[€※]	−0.035 ± 0.002[§€]	−0.082 ± 0.010[€※]	0.005 ± 0.006[€]	**1563.0 ± 96.9.1**[§€]
B + W + D	**1746.5 ± 60.8**[§]	193.7 ± 4.9[§]	1377.5 ± 42.1[§]	175.3 ± 17.1[§]	**−0.053 ± 0.043**[§€]	−0.040 ± 0.003[€]	−0.067 ± 0.023[§€]	0.053 ± 0.019[§]	**1744.6 ± 61.8**[§]

Data of the entire growing season (G) are marked in bold.
[§] The same letter in a column denotes non-significant differences among treatments from *post hoc* comparison of mean tests at $P \geq 0.05$.
[€] The sites of B, B + W, B + D, B + W + D represent the burned, burned + warm, burned + dry and burned + warm + dry sites.

mature forest. Furthermore, the global warming potential of total C flux in the burned + warm, burned + dry and burned + warm + dry plots was 46.3%, 52.5% and 70.2% higher than that in the mature forest, respectively (Table 4).

4. Discussion

4.1. Responses of soil CO_2 fluxes to wildfire, warming and drying

Wildfire is known to be a widespread disturbance influencing the C budget of boreal forest ecosystems (Balshi et al., 2010; O'Neill et al., 2003; Turetsky et al., 2011), especially under a warmer climate (Abbott et al., 2016). Wildfire initiates new successional regimes in ecosystems, and its influences last several decades (Kurz et al., 2013). We found that the early successional boreal forest 7–8 years after a fire had a higher soil CO_2 flux than the mature forest, which is consistent with previous observations in the boreal region (Burke et al., 1997; O'Neill et al., 2003; Song et al., 2017). One possible explanation for this result is that the post-fire forest has a higher quality of detrital input because of the invasion of more deciduous species and ground vegetation (Zehetgruber et al., 2017), which might enhance decomposition. This speculation was corroborated by the higher soil DTN and enzymatic activities in the burned sites (Fig. 1), indicating higher soil nutrient availability and stronger metabolic activity during the early succession following fire (Jiang et al., 2016), although there was less soil MBC and MBN in the burned forest. Moreover, the higher soil CO_2 flux in the post-fire site might be partly from the significantly increased active layer depth following fire (Mack et al., 2011), which made soil organic C that was originally locked in the permafrost layer available for microbial decomposition (Dorrepaal et al., 2009), potentially leading to a higher soil CO_2 release.

Soil CO_2 flux of the boreal forest following fire will be further enhanced by a warming climate. Allison et al. (2010) found that the warming response of post-fire boreal forests was very weak in a region lacking permafrost, indicating that the increased soil CO_2 emissions in the burned + warm plots in our study might be related to the increased permafrost thaw. The increased active layer in the burned + warm plots with a weaker warming extent indicated that permafrost might be more sensitive to the climate warming following fire (Brown et al., 2015). As mentioned above, there were more soil nutrient availability and enzymatic activities following fire. So, soil CO_2 flux in burned + dry plots would be increased by their drier and warmer soil condition through increasing decomposition of soil C, and not be constrained by the depletion of labile C substrates (Allison et al., 2010). Therefore, we expected that the soil CO_2 flux would be highest in the burned+warm+dry plots with higher soil temperature under more oxic condition, showing a synergistic effect between warming and drying. In this study, the combined warming and drying treatment did increase cumulative soil CO_2 emissions by 34.2% of the burned forest. Thus, our results exhibited an interaction between fire and the response of soil CO_2 flux to climate warming and soil drying through the increase in soil nutrient availability and permafrost thaw following fire (Brown et al., 2015; Jiang et al., 2016; Mack et al., 2011). However, the temperature sensitivities of post-fire forest were decreased by the warming and drying treatments, which might result from the decrease in soil moisture (Kim and Tanaka, 2003; Kim, 2015; Riveros-Iregui et al., 2007) and the increase in soil temperature (Kirschbaum, 1995).

Although there were no significant differences in MBC and DOC contents among the treatments of burned, burned + warm, burned + dry, and burned + warm + dry, evidence of older $^{14}CO_2$ in the soil pore space in the dry plots was found by Natali et al. (2015), suggesting an additional input of older microbial-respired CO_2 upon soil drying. However, the burned + dry plots had lower enzymatic activity in this study, which was similar to the result in peatlands and was probably due to drought stress (Christiansen et al., 2016; Wiedermann et al., 2017), as indicated by the deeper fine root distribution (Supplementary Fig. E).

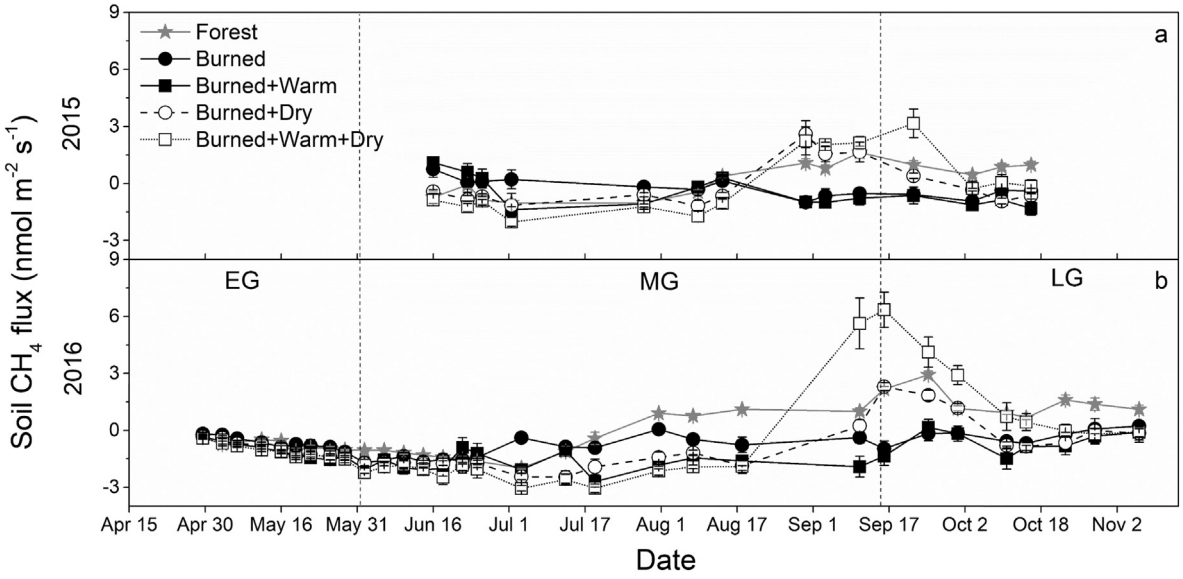

Fig. 3. Seasonal variation of soil CH_4 flux in the forest, burned, burned + warm, burned + dry and burned + warm + dry sites in 2015 (a) and 2016 (b). Error bars represent standard error of the mean (n = 5); EG, MG and LG represent the early, middle and late growing season, respectively.

There appears to be a contradiction between the higher microbial decomposition and lower enzymatic activities in our study. Firstly, as many temporally fluctuating biotic and abiotic factors can influence enzyme production and function (Kivlin and Treseder, 2014), the point measurements of enzymatic activities did not capture the long term microbial decomposition processes (Wiedermann et al., 2017). Meanwhile, the enzymatic activities were measured only in the topsoil, whereas CO_2 could also be produced in the deeper soil.

4.2. Responses of soil CH_4 fluxes to wildfire, warming and drying

Coniferous-forested wetlands in Northeast China, which occupy a large wetland area in this region, were observed to be weak sinks or sources of atmospheric CH_4 (Song et al., 2017; Sun et al., 2011). In the present study, the mature forest that acted as a weak source of CH_4 to the atmosphere was changed to a weak sink by the fire disturbance. This result was closely related to the deeper water table in the burned plots, which led to an increased zone of CH_4 oxidation and consequently a decrease in CH_4 emissions (Lawrence et al., 2015; Turetsky et al., 2008). Moreover, the higher soil CH_4 flux in the mature forest might be associated with their higher soil MBC and DOC content which had a positive relationship with soil CH_4 fluxes (Supplementary Table B). At the same time, there was no peak of CH_4 emission in September in the post-fire forest based on the seasonal variation of soil CH_4 flux (Fig. 3). So, the post-fire forest had a lower soil CH_4 emission than the mature forest.

When the burned plots experienced a warmer climate, the increased zone of soil CH_4 oxidation led to higher CH_4 uptake and formed an enhanced sink of atmospheric CH_4 due to the increased maximum thaw depth (Supplementary Table A; Jørgensen et al., 2015). However, accompanying the warming, soil water, the most important factor affecting the soil CH_4 flux, may decrease as the water table declines as a result of permafrost thawing (Lawrence et al., 2015). After drying, the soil CH_4 flux showed a significant temporal pattern with a peak in emissions in late September and the burned + dry and burned + warm + dry plots exhibited lower mean CH_4 uptake throughout the growing season. Thus, the warming and drying treatments exhibited interactive effects. The lower soil CH_4 uptake following drying may also be driven by the increased inputs of labile C available to methanogens (Jiang et al., 2016; Olefeldt et al., 2013) and changes in the methanogen and methane-oxidizing bacterial communities (Mastepanov et al., 2008; Peltoniemi et al., 2016), as expressed by the increased dissolved organic C and changes in the MBC/MBN ratio in our study (Fig. 1). Seasonal soil CH_4 emission peaks in the late autumn and early winter have also been observed in the tundra (Mastepanov et al., 2008), and the magnitude of these emissions were found to be approximately equal to the amount of CH_4 emitted during the entire summer season, thus representing an important component of CH_4 emissions from high latitudes. In contrast, the CH_4 emission in wetlands was found to occur during the spring thaw period (Song et al., 2012). In the permafrost region, the CH_4 emission peaks are related to high CH_4 concentrations in the upper permafrost layer (Miao et al., 2012) formed

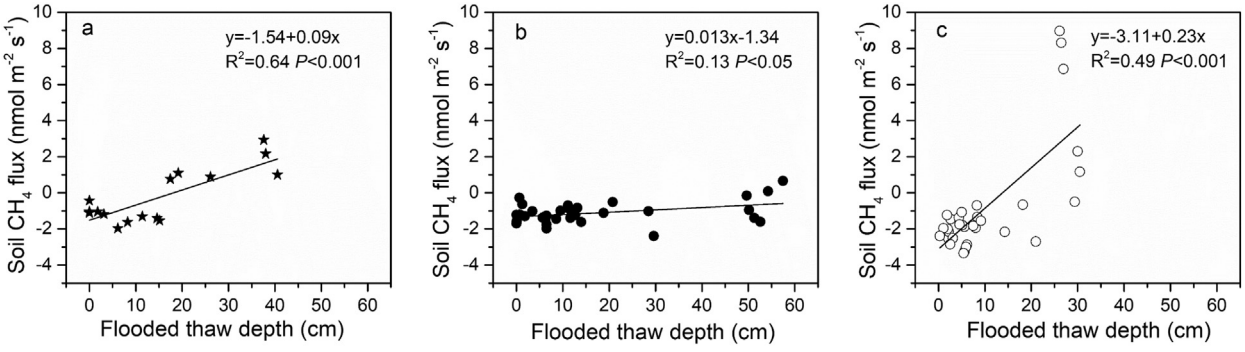

Fig. 4. Relationship between the flooded thaw depth (distance from water table to permafrost table surface) and soil CH_4 flux in the forest (a; n = 16), burned and burned + warm sites (b; n = 32) and burned + dry and burned + warm + dry sites (c; n = 32).

by modern methanogenesis by cold-adapted methanogenic archaea in the permafrost soil (Wagner et al., 2007) and trapped CH_4 formed in the unfrozen active layer during the previous winter (Miao et al., 2012). When the active layer reached the layer with high CH_4 concentrations and a shallower water table (associated with lower CH_4 consumption) was present at the same time, the soil CH_4 flux peaked. As the CH_4 oxidation rates were not primarily diffusion limited in the soils after the drying treatment, the soil CH_4 flux was significantly correlated to the flooded thaw depth for CH_4 production ($R^2 = 0.49$; Fig. 4c), leading to an obvious seasonal variation. In contrast, this correlation between soil CH_4 flux and flooded thaw depth was weaker in the no-drying condition ($R^2 = 0.13$; Fig. 4b), accounting for the lack of distinct seasonal variation in the no-drying burned plots (burned plots and burned + warm plots). However, most previous studies predicted that soil drainage would lead to a decrease in soil CH_4 emissions in regions the soil acts as a source of CH_4 to the atmosphere (Lawrence et al., 2015; Merbold et al., 2009; Sturtevant et al., 2012). Therefore, a drier soil, particularly a drier soil under a warmer climate, might have the potential to change the weak atmospheric CH_4 sinks from a sink to a source of CH_4.

4.3. Responses of soil C fluxes in different periods

In present study, soil CO_2 fluxes seasonally varied. Accordingly, the cumulative soil CO_2 fluxes in the burned + warm plots were 21.3%, 10.2% and 63.9% higher than those in the burned plots in the EG, MG and LG periods, respectively, showing seasonal differences. This stronger treatment effect on soil CO_2 emissions in the late growing season was probably from the gradually accumulated energy from the warming treatment throughout the growing season in the late growing season. Additionally, in the late growing season, the treatment effects on the soil dynamics by vegetation growth changes were the most obvious. Similarly, the burned + dry and the burned + warm + dry plots also showed the strongest increases in cumulative soil CO_2 emissions in the late growing season, highlighting the important role of the late growing season in the entire season CO_2 flux budget (Chen et al., 2017).

In the late growing season, the burned + dry and burned + warm + dry plots exhibited net cumulative soil CH_4 emissions, whereas there were soil CH_4 uptakes in the burned and burned+ warm plots (Table 4). This result was because the cumulative uptake of CH_4 was offset by the soil CH_4 emission peak in September (Mastepanov et al., 2008; Miao et al., 2012). As a net release of CH_4 to the atmosphere and the highest combined effects of warming and drying on the soil CH_4 flux occurred in the late growing season (Table 4), the potential of changing this region from a weak sink to a source of CH_4 mostly occurred during the late growing season. Therefore, the late growing season, with the associated higher water table, was critical for soil CH_4 flux regime (Mastepanov et al., 2008).

4.4. Responses of global warming potentials of soil total C flux to wildfire, warming and drying

GWP was used to take the competing impacts of soil CO_2 and CH_4 fluxes together. The post-fire boreal forest recovered from fire 7–8 years had a GWP that was 26.6% higher than that of the mature forest in the growing season. Coupled with the decreased net primary production, the young post-fire boreal forest is more likely to act as a C source to the atmosphere (Goulden et al., 2011; Kurz et al., 2013), indicating a possible change in the C balance in the boreal region. Moreover, early successional systems are more sensitive to perturbations than mature systems based on the feature of ecosystem (Kröel-Dulay et al., 2015). This conclusion was confirmed by the significantly higher temperature sensitivity of the soil CO_2 emissions in the burned plots in our results (Supplementary Fig. F), primarily due to the thawing of permafrost and increase in soil moisture (Song et al., 2017). Thus, the post-fire boreal forest will likely have stronger feedbacks to climate warming than the unburned forests. These responses to climate change are of vital importance because of the increase in fire frequency and intensity (Abbott et al., 2016).

Warming and drying further increased the GWP of soil total C fluxes from the burned site. So, our study area, which is experiencing warming and drying climate trend (Sun et al., 2005), will likely express higher warming potential of greenhouse gas emissions, particularly in the post-fire forest. The burned site experiencing the combination of warming and drying had a 70.2% higher GWP than the undisturbed boreal forest. This process, coupled with the large C stocks in boreal soil (Bradshaw and Warkentin, 2015), may produce a strong positive feedback in the global C cycle.

In the permafrost ecosystem, one major uncertainty in determining the climate forcing impact is understanding the relative magnitudes of the effects of shifting subsurface hydrology *versus* increasing temperatures on greenhouse gas releases (Schädel et al., 2016), which might be related to the form of the soil C losses. When the soil CH_4 emissions contribute to a high proportion of the soil C emissions, Lawrence et al. (2015) predicted that the drying following the permafrost thaw will weaken the soil C flux (CO_2 and CH_4) by 50% due to the strong suppression of CH_4 emissions, similar to the results of an artificial drainage experiment in the tundra ecosystem (Merbold et al., 2009; Turetsky et al., 2008). However, in our study region which acted as weak sink of CH_4, the decreases of cumulative soil CH_4 flux under warming and drying treatments did not weaken the total C emissions that much due to their low proportions. Therefore, the form of C fluxes (the relative proportion of CO_2 and CH_4) are critical for understanding the response of the total soil C flux to the climate changes.

4.5. Uncertainties of this experiments

Some uncertainties that may interfere with the experiment are listed here. First of all, the simulated warming treatment by OTCs just increased the air temperature by approximate 1 °C, but did not increase the soil temperature at a depth of 5 cm (Table 1). This was a relatively low warming extent. Therefore, the differences of soil CO_2 and CH_4 fluxes between warming treatments cannot be explained by a weaker warming effect, but by the interaction of fire and permafrost degradation (Brown et al., 2015) and the increase of soil nutrient availability (Jiang et al., 2016). Moreover, there were not warming and drying treatments conducted in the mature forests. Therefore, we cannot obtain the real interaction between the fire and climate changes such as warming and drying. However, our situ experiment can still present us some important information of how soil CO_2 and CH_4 fluxes in the young post-fire boreal forest locating in permafrost regions responded to the climate changes.

5. Conclusions

A boreal forest recovered form wildfire 7–8 years had higher soil CO_2 flux than the mature forest, and the soil CO_2 flux in the post-fire forest was further increased under warmer climate and dryer soil condition. Moreover, the positive response of soil CO_2 flux to warming was further amplified by drier soil conditions. However, fire disturbance changed the boreal forest from a weak source of CH_4 to a weak sink that was further increased by warming or drying treatments. But the interaction of warming and drying led to a decrease in the soil CH_4 uptakes. Therefore, climate warming and soil drying, especially their combination, increased the soil total C flux in post-fire boreal forests underlain by permafrost. As early successional ecosystems more likely to act as sources of C to the atmosphere due to the increased soil C decomposition and decreased net primary production after fires, their positive responses of soil C emissions to warming and drying might drive much stronger positive feedbacks on climate than the mature forests. Coupled with an increase in fire frequency, the C balance of early successional ecosystems might play a more important role in the future global C budget.

Moreover, the results of different seasonal periods highlighted the role of changes in permafrost thawing and soil water conditions on both the magnitude and the form of C losses and underlined the importance of the late growing season.

Acknowledgements

This work was supported by the National Key Basic Research Program of China [grant number 2013CBA01807] and the National Natural Science Foundation of China [grant numbers 91547203; 41271224; 41671206].

Appendix A. Supplementary data

Supplementary data to this article can be found online at https://doi.org/10.1016/j.scitotenv.2018.07.014.

References

Abbott, B.W., Jones, J.B., Schuur, E.A.G., Iii, F.S.C., Bowden, W.B., Bretharte, M.S., Epstein, H.E., Flannigan, M.D., Harms, T.K., Hollingsworth, T.N., 2016. Biomass offsets little or none of permafrost carbon release from soils, streams, and wildfire: an expert assessment. Environ. Res. Lett. 11, 034014.

Allison, S.D., Mcguire, K.L., Treseder, K.K., 2010. Resistance of microbial and soil properties to warming treatment seven years after boreal fire. Soil Biol. Biochem. 42, 1872–1878.

Amiro, B.D., Barr, A.G., Barr, J.G., Black, T.A., Bracho, R., Brown, M., Chen, J., Clark, K.L., Davis, K.J., Desai, A.R., Dore, S., Engel, V., Fuentes, J.D., Goldstein, A.H., Goulden, M.L., Kolb, T.E., Lavigne, M.B., Law, B.E., Margolis, H.A., Martin, T., Mccaughey, J.H., Misson, L., Montes-Hulu, M., Noormets, A., Randerson, J.T., Starr, G., Xiao, J., 2015. Ecosystem carbon dioxide fluxes after disturbance in forests of North America. Journal of Geophysical Research Biogeosciences 115. https://doi.org/10.1029/2010JG001390.

Avis, C.A., Weaver, A.J., Meissner, K.J., 2011. Reduction in areal extent of high-latitude wetlands in response to permafrost thaw. Nat. Geosci. 4, 444–448.

Balshi, M.S., Mcguire, A.D., Duffy, P., Flannigan, M., Kicklighter, D.W., Melillo, J., 2010. Vulnerability of carbon storage in North American boreal forests to wildfires during the 21st century. Glob. Chang. Biol. 15, 1491–1510.

Bintanja, R., Selten, F.M., 2014. Future increases in Arctic precipitation linked to local evaporation and sea-ice retreat. Nature 509, 479–482.

Bockheim, J.G., 2015. Cryopedology. Springer Press, Heidelberg-New York-Dordrecht-London.

Bradshaw, C.J.A., Warkentin, I.G., 2015. Global estimates of boreal forest carbon stocks and flux. Glob. Planet. Chang. 128, 24–30.

Brown, D.R.N., Torre, J.M., Douglas, T.A., Romanovsky, V.E., Knut, K., Christopher, H., Euskirchen, E.S., Ruess, R.W., 2015. Interactive effects of wildfire and climate on permafrost degradation in Alaskan lowland forests. J. Geophys. Res. Biogeosci. 120, 1619–1637.

Burke, R.A., Zepp, R.G., Tarr, M.A., Miller, W.L., Stocks, B.J., 1997. Effect of fire on soil-atmosphere exchange of methane and carbon dioxide in Canadian boreal forest sites. J. Geophys. Res. Atmos. 1022, 29289–29300.

Chen, X., Wang, G., Zhang, T., Mao, T., Wei, D., Song, C., Hu, Z., Huang, K., 2017. Effects of warming and nitrogen fertilization on GHG flux in an alpine swamp meadow of a permafrost region. Sci. Total Environ. 601-602, 1389–1399.

Chivers, M.R., Turetsky, M.R., Waddington, J.M., Harden, J.W., Mcguire, A.D., 2009. Effects of experimental water table and temperature manipulations on ecosystem CO_2 fluxes in an Alaskan rich fen. Ecosystems 12, 1329–1342.

Christiansen, C.T., Haugwitz, M.S., Priemé, A., Nielsen, C.S., Elberling, B., Michelsen, A., Grogan, P., Blok, D., 2016. Enhanced summer warming reduces fungal decomposer diversity and litter mass loss more strongly in dry than in wet tundra. Glob. Chang. Biol. 23, 406.

Dorrepaal, E., Toet, S., Logtestijn, R.S.P.V., Swart, E., Weg, M.J.V.D., Callaghan, T.V., Aerts, R., 2009. Carbon respiration from subsurface peat accelerated by climate warming in the subarctic. Nature 460, 616–619.

Eivazi, F., Tabatabai, M.A., 1988. Glucosidases and galactosidases in soils. Soil Biol. Biochem. 20, 601–606.

Fang, J., Chen, A., Peng, C., Zhao, S., Ci, L., 2001. Changes in forest biomass carbon storage in China between 1949 and 1998. Science 292, 2320–2322.

Goulden, M.L., Mcmillan, A.M.S., Winston, G.C., Rocha, A.V., Manies, K.L., Harden, J.W., Bond-Lamberty, B.P., 2011. Patterns of NPP, GPP, respiration, and NEP during boreal forest succession. Glob. Chang. Biol. 17, 855–871.

Guan, S., Zhang, D., Zhang, Z., 1986. Soil Enzyme and Its Research Methods. Agricultural (in Chinese), Beijing. pp. 291–294.

Held, I.M., Soden, B.J., 2006. Robust responses of the hydrological cycle to global warming. J. Clim. 19, 5686–5699.

Hugelius, G., Strauss, J., Zubrzycki, S., Harden, J.W., Schuur, E.A.G., Ping, C.L., Schirrmeister, L., Grosse, G., Michaelson, G.J., Koven, C.D., 2014. Estimated stocks of circumpolar permafrost carbon with quantified uncertainty ranges and identified data gaps. Biogeosciences 11, 6573–6593.

IPCC, 2013. Contribution of working group I to the fifth assessment report of the intergovernmental panel on climate change. The Physical Science Basis.

Jiang, Y., Rastetter, E.B., Shaver, G.R., Rocha, A.V., Zhuang, Q., Kwiatkowski, B.L., 2016. Modeling long-term changes in tundra carbon balance following wildfire, climate change, and potential nutrient addition. Ecol. Appl. 27, 105–117.

Jørgensen, C.J., Johansen, K.M.L., Westergaardnielsen, A., Bo, E., 2015. Net regional methane sink in High Arctic soils of northeast Greenland. Nat. Geosci. 8, 20–23.

Jorgenson, M.T., Racine, C.H., Walters, J.C., Osterkamp, T.E., 2001. Permafrost degradation and ecological changes associated with a warming climate in central Alaska. Clim. Chang. 48, 551–579.

Kim, Y., 2015. Effect of thaw depth on fluxes of CO_2 and CH_4 in manipulated Arctic coastal tundra of Barrow, Alaska. Sci. Total Environ. 505, 385–389.

Kim, Y., Tanaka, N., 2003. Effect of forest fire on the fluxes of CO_2, CH_4 and N_2O in boreal forest soils, interior Alaska. J. Geophys. Res. Atmos. 108 (FFR 10-11–FFR 10-12).

Kirschbaum, M.U.F., 1995. The temperature dependence of soil organic matter decomposition, and the effect of global warming on soil organic C storage. Soil Biol. Biochem. 27, 753–760.

Kivlin, S.N., Treseder, K.K., 2014. Soil extracellular enzyme activities correspond with abiotic factors more than fungal community composition. Biogeochemistry 117, 23–37.

Kröel-Dulay, G., Ransijn, J., Schmidt, I.K., Beier, C., De, A.P., De, D.G., Dukes, J.S., Emmett, B., Estiarte, M., Garadnai, J., 2015. Increased sensitivity to climate change in disturbed ecosystems. Nat. Commun. 6, 6682.

Kurz, W.A., Shaw, C.H., Boisvenue, C., Stinson, G., Metsaranta, J., Leckie, D., Dyk, A., Smyth, C., Neilson, E.T., 2013. Carbon in Canada's boreal forest-a synthesis. Environ. Rev. 21, 260–292.

Kwon, M.J., Beulig, F., Ilie, I., Wildner, M., Küsel, K., Merbold, L., Mahecha, M.D., Zimov, N., Zimov, S.A., Heimann, M., 2017. Plants, microorganisms, and soil temperatures contribute to a decrease in methane fluxes on a drained Arctic floodplain. Glob. Chang. Biol. 23, 2396–2412 (2317).

Lawrence, D.M., Slater, A.G., Swenson, S.C., 2012. Simulation of present-day and future permafrost and seasonally frozen ground conditions in CCSM4. J. Clim. 25, 2207–2225.

Lawrence, D.M., Koven, C.D., Swenson, S.C., Riley, W.J., Slater, A.G., 2015. Permafrost thaw and resulting soil moisture changes regulate projected high-latitude CO_2 and CH_4 emissions. Environ. Res. Lett. 10, 094011.

Lee, K.H., Jose, S., 2003. Soil respiration, fine root production, and microbial biomass in cottonwood and loblolly pine plantations along a nitrogen fertilization gradient. For. Ecol. Manag. 185, 263–273.

Lloyd, J., Taylor, J.A., 1994. On the temperature dependence of soil respiration. Funct. Ecol. 8, 315–323.

Macdougall, A.H., Avis, C.A., Weaver, A.J., 2012. Significant contribution to climate warming from the permafrost carbon feedback. Nat. Geosci. 5, 719–721.

Mack, M.C., Bret-Harte, M.S., Hollingsworth, T.N., Jandt, R.R., Schuur, E.A., Shaver, G.R., Verbyla, D.L., 2011. Carbon loss from an unprecedented arctic tundra wildfire. Nature 475, 489–492.

Marion, G.M., Henry, G.H.R., Freckman, D.W., Johnstone, J., Jones, G., Jones, M.H., Lévesque, E., Molau, U., Mølgaard, P., Parsons, A.N., 1997. Open-top designs for manipulating field temperature in high latitude ecosystems. Glob. Chang. Biol. 3, 20–32.

Mastepanov, M., Sigsgaard, C., Dlugokencky, E.J., Houweling, S., Ström, L., Tamstorf, M.P., Christensen, T.R., 2008. Large tundra methane burst during onset of freezing. Nature 456, 628–630.

Merbold, L., Kutsch, W.L., Corradi, C., Kolle, O., Rebmann, C., Stoy, P.C., Zimov, S.A., Schulze, E.D., 2009. Artificial drainage and associated carbon fluxes (CO_2/CH_4) in a tundra ecosystem. Glob. Chang. Biol. 15, 2599–2614.

Miao, Y., Song, C., Sun, L., Wang, X., Meng, H., Mao, R., 2012. Growing season methane emission from a boreal peatland in the continuous permafrost zone of Northeast China: effects of active layer depth and vegetation. Biogeosciences 9, 4455–4464.

Morgenstern, A., Ulrich, M., Günther, F., Roessler, S., Fedorova, I.V., Rudaya, N.A., Wetterich, S., Boike, J., Schirrmeister, L., 2013. Evolution of thermokarst in east Siberian ice-rich permafrost: a case study. Geomorphology 201, 363–379.

Natali, S.M., Schuur, E.A.G., Mauritz, M., Schade, J.D., Celis, G., Crummer, K.G., Johnston, C., Krapek, J., Pegoraro, E., Salmon, V.G., 2015. Permafrost thaw and soil moisture driving CO_2 and CH_4 release from upland tundra. J. Geophys. Res. Biogeosci. 120, 525–537.

O'Donnell, J.A., Jorgenson, M.T., Harden, J.W., Mcguire, A.D., Kanevskiy, M.Z., Wickland, K.P., 2012. The effects of permafrost thaw on soil hydrologic, thermal, and carbon dynamics in an Alaskan peatland. Ecosystems 15, 213–229.

Olefeldt, D., Turetsky, M.R., Crill, P.M., Mcguire, A.D., 2013. Environmental and physical controls on northern terrestrial methane emissions across permafrost zones. Glob. Chang. Biol. 19, 589–603.

O'Neill, K.P., Kasischke, E.S., Richter, D.D., 2003. Seasonal and decadal patterns of soil carbon uptake and emission along an age sequence of burned black spruce stands in interior Alaska. J. Geophys. Res. Atmos. 108 (FFR 11-11–FFR 11-15).

Overland, J.E., 2014. Future Arctic climate changes: adaptation and mitigation time scales. Earths Futur. 2, 68–74.

Peltoniemi, K., Laiho, R., Juottonen, H., Bodrossy, L., Kell, D.K., Minkkinen, K., Mäkiranta, P., Mehtätalo, L., Penttilä, T., Siljanen, H.M.P., 2016. Responses of methanogenic and methanotrophic communities to warming in varying moisture regimes of two boreal fens. Soil Biol. Biochem. 97, 144–156.

Peng, C.H., Zhou, X.L., Zhao, S.Q., Wang, X.P., Zhu, B., Shilong, P., Fang, J.Y., 2009. Quantifying the response of forest carbon balance to future climate change in Northeastern China: model validation and prediction. Glob. Planet. Chang. 66, 179–194.

Riveros-Iregui, D.A., Emanuel, R.E., Muth, D.J., Mcglynn, B.L., Epstein, H.E., Welsch, D.L., Pacific, V.J., Wraith, J.M., 2007. Diurnal hysteresis between soil CO_2 and soil temperature is controlled by soil water content. Geophys. Res. Lett. 34 (138–138).

Schädel, C., Bader, M.K.F., Schuur, E.A.G., Biasi, C., Bracho, R., Čapek, P., Baets, S.D., Diáková, K., Ernakovich, J., Estoparagones, C., 2016. Potential carbon emissions dominated by carbon dioxide from thawed permafrost soils. Nat. Clim. Chang. 6.

Schuur, E.A.G., Bockheim, J., Canadell, J.G., Euskirchen, E., Field, C.B., Goryachkin, S.V., Hagemann, S., Kuhry, P., Lafleur, P.M., Lee, H., 2008. Vulnerability of permafrost carbon to climate change: implications for the global carbon cycle. Bioscience 58, 701–714.

Schuur, E.A.G., Abbott, B.W., Bowden, W.B., Brovkin, V., Camill, P., Canadell, J.G., Chanton, J.P., Chapin, F.S., Christensen, T.R., Ciais, P., 2013. Expert assessment of vulnerability of permafrost carbon to climate change. Clim. Chang. 119, 359–374.

Slater, A.G., Lawrence, D.M., 2013. Diagnosing present and future permafrost from climate models. J. Clim. 26, 5608–5623.

Song, C., Xu, X., Sun, X., Tian, H., Sun, L., Miao, Y., Wang, X., Guo, Y., 2012. Large methane emission upon spring thaw from natural wetlands in the northern permafrost region. Environ. Res. Lett. 7, 34009–34016 (34008).

Song, X., Wang, G., Ran, F., Chang, R., Song, C., Xiao, Y., 2017. Effects of topography and fire on soil CO_2 and CH_4 flux in boreal forest underlain by permafrost in northeast China. Ecol. Eng. 106, 35–43.

Sturtevant, C.S., Oechel, W.C., Zona, D., Kim, Y., Emerson, C.E., 2012. Soil moisture control over autumn season methane flux, Arctic Coastal Plain of Alaska. Biogeosciences 9, 1423–1440.

Sun, F., Yang, S., Chen, P., 2005. Climatic warming-drying trend in Northeastern China during the last 44 years and its effects. Chin. J. Ecol. 24, 751–755,762.

Sun, X., Mu, C., Song, C., 2011. Seasonal and spatial variations of methane emissions from montane wetlands in Northeast China. Atmos. Environ. 45, 1809–1816.

Tarnocai, C., Canadell, J.G., Schuur, E.A.G., Kuhry, P., Mazhitova, G., Zimov, S., 2009. Soil organic carbon pools in the northern circumpolar permafrost region. Glob. Biogeochem. Cycles 23, 2607–2617.

Turetsky, M.R., Treat, C.C., Waldrop, M.P., Waddington, J.M., Harden, J.W., Mcguire, A.D., 2008. Short-term response of methane fluxes and methanogen activity to water table and soil warming manipulations in an Alaskan peatland. J. Geophys. Res. Biogeosci. 113, 119–128.

Turetsky, M.R., Kane, E.S., Harden, J.W., Ottmar, R.D., Manies, K.L., Hoy, E., Kasischke, E.S., 2011. Recent acceleration of biomass burning and carbon losses in Alaskan forests and peatlands. Nat. Geosci. 4, 27–31.

Updegraff, K., Bridgham, S.D., Pastor, J., Weishampel, P., Harth, C., 2001. Response of CO_2 and CH_4 emissions from peatlands to warming and water table manipulation. Ecol. Appl. 11, 311–326.

Wagner, D., Gattinger, A., Embacher, A., Pfeiffer, E., Schloter, M., Lipski, A., 2007. Methanogenic activity and biomass in Holocene permafrost deposits of the Lena Delta, Siberian Arctic and its implication for the global methane budget. Glob. Chang. Biol. 13, 1089–1099.

Wang, C., Gower, S.T., Wang, Y., Zhao, H., Ping, Y., Bond-Lamberty, B.P., 2001. The influence of fire on carbon distribution and net primary production of boreal *Larix gmelinii* forests in north-eastern China. Glob. Chang. Biol. 7, 719–730.

Webster, K.L., Creed, I.F., Bourbonnière, R.A., Beall, F.D., 2008. Controls on the heterogeneity of soil respiration in a tolerant hardwood forest. J. Geophys. Res. Biogeosci. 113, 851–854.

Wiedermann, M.M., Kane, E.S., Potvin, L.R., Lilleskov, E.A., 2017. Interactive plant functional group and water table effects on decomposition and extracellular enzyme activity in *Sphagnum* peatlands. Soil Biol. Biochem. 108, 1–8.

Wu, J., Joergensen, R.G., Pommerening, B., Chaussod, R., Brookes, P.C., 1990. Measurement of soil microbial biomass C by fumigation-extraction-an automated procedure. Soil Biol. Biochem. 22, 1167–1169.

Zehetgruber, B., Kobler, J., Dirnböck, T., Jandl, R., Seidl, R., Schindlbacher, A., 2017. Intensive ground vegetation growth mitigates the carbon loss after forest disturbance. Plant Soil 420, 1–14.

Zhang, T., Wang, G., Yang, Y., Mao, T., Chen, X., 2015. Non-growing season soil CO_2 flux and its contribution to annual soil CO_2 emissions in two typical grasslands in the permafrost region of the Qinghai-Tibet Plateau. Eur. J. Soil Biol. 71, 45–52.